Measurement of the Thermal Characteristics of Finned-tube Heat Exchanger Fin by Using the Liquid Crystal Technique

Hie Chan Kang* and Moo Hwan Kim**

Key words: Heat exchanger, Heat transfer, Conduction, Fin efficiency, Liquid crystal

Abstract

This study deals with the thermal characteristics of finned-tube heat exchanger having two rows used in the air-conditioning application. Pressure drop and heat transfer coefficient were measured by using the three times models of plain fin and compared with the theory. Also the temperature distribution and heat conduction in the fin was measured by using the liquid crystal method. The surface temperature of rear row was nearly constant, and heat conduction in the fin was stronger near the front row than the rear row.

Nomenclature

A	: area [m^2]
A_c	: minimum cross sectional area [m^2]
A_{fr}	: frontal area [m^2]
A_i	: tube inside area [m^2]
c_p	: heat capacity [J/kg℃]
D	: tube diameter [m]
f	: friction factor
G_c	: mass velocity at minimum cross section, ρV_c [kg/m$^2\cdot$s]
h	: heat transfer coefficient [W/m^2℃]
h_i	: heat transfer coefficient of tube inside [W/m^2℃]
j	: Colburn j factor
n	: scale factor
P_f	: fin pitch [m]
P_t	: tube pitch [m]
Pr	: Prandtl number, ν/α
Q	: heat transfer rate per unit fin [W]
Re	: Reynolds number, $G_c D/\mu$
T	: temperature [℃]
t	: fin thickness [m]
ΔT_{LM}	: logarithmic temperature difference [℃]
U	: overall heat transfer coefficient [W/m^2℃]
V_c	: velocity at minimum cross section [m/s] or volume inside fin [m^3]
V_{fr}	: frontal velocity [m/s]

Greek letters

α	: thermal diffusivity [m^2/s]

* Faculty of Mechanical Engineering, Kunsan National University, Kunsan 573-701, Korea
** Department of Mechanical Engineering, POSTECH, Pohang 790-784, Korea

η : surface efficiency

μ : viscosity [kg/m · s]

ρ : density [kg/m^3]

Subcripts

ex : exit

in : inlet

tot : fin and tube

w : wall

1. Introduction

The finned-tube heat exchanger has been widely used in air-conditioning applications for many years. The enhancement has been focused on increasing performance in heat transfer, decreasing pressure drop in the air side and the size of the heat exchanger. To achieve this goal, it is necessary to reduce the air-side thermal resistance, since the resistance covers more than 70% of the total thermal resistance that consists of the air-side, the refrigerant-side and the contact resistance. A lot of studies have been performed to find the enhanced fin geometries such as the plain fin, offset strip fin, louver fin, convex louver fin and wavy fin etc. However there is not much work on the alignment of strips or enhanced surfaces on the fin to reduce the pressure drop.

Various types of fins have been proposed to get a high performance heat exchanger. One method is to promote turbulence and increase the flow length of air flow by using the wavy or corrugated fin geometries. Baggio and Fornasieri[1] reported that the increase in heat transfer rate of a corrugated fin over that of a plain fin is of the order of about 20% at the same fan power. A widely exploited way of improving the heat transfer coefficient relies on the use of interrupted surfaces. High heat transfer performance can be achieved at every interrupted surface in the strip fins. Therefore the average heat transfer coefficient is increased.

Goldstein and Sparrow[2] used the naphthalene sublimation. Beecher and Fagan,[3] Ali and Ramadhyani[4] tested their heat exchanger as uniform surface temperature condition. Ito et al.[5] applied the constant heat flux condition. However it is not easy to find experimental data for the fin temperature distribution. Kang and Kim[6] proposed the scaled-up model test and showed that it could be very powerful technique in the development of fins. They showed that their technique could replace the full-scale test in the performance evaluation, moreover, save great deal of time and money comparing the full-scale test.

Kim[7] successfully applied a liquid crystal method to investigate the flow and heat transfer characteristics of an impinging jet. Bunker[8] and Camci et al.[9] proposed calibration methods to transform the measured color to the temperature in the use of the liquid crystal.

This study was an extension of the scaled-up model test developed by Kang and Kim[6] to measure the fin temperature. The liquid crystal method was proposed for the finned-tube heat exchanger having plane fin and two rows. The experimental technique is developed and quantitative data are provided.

2. Experimental apparatus and method

2.1 Similarity

It would take very much time and money to make a prototype heat exchanger for test purposes. Making highly accurate fin dies is very expensive. Additionally we would have to pay for making fin collars and the tube expansion to bond the fin and tube. We can greatly reduce the cost if we only concentrate on the air side performance of heat exchanger. The details are discussed in the reference of Kang

Table 1 Comparison of parameters between prototype and scale-up model heat exchangers tested in the present work

Parameter	Prototype HEX	Model type HEX
fin material	aluminum	aluminum
scale factor	1	3 (n)
thermal conductivity (W/m℃)	222	222
fin thickness (mm)	0.1	0.3 (n)
pressure drop*	1	0.111 ($1/n^2$)
heat transfer coefficient*	1	3 (1/n)
Re, Pr, f, j	1	1

* Means the ratio of values of model type to those of prototype.

and Kim.[6] The present experiment was conducted for three times enlarged model with the same geometric configuration. We can obtain similarity between the model and the prototype if the Re, Pr numbers and non-dimensional fin thickness are the same. Applying the same boundary conditions, we could get the same f and j factors and the fin efficiency in the model test. For complete similarity, we must maintain similar temperature distribution in the fin. Table 1 shows the relation of parameters between prototype and model heat exchangers.

2.2 Experimental apparatus

A low speed wind tunnel as shown in Fig. 1 was required to satisfy the actual operation condition. The wind tunnel was a suction and open loop type. It consisted of a fan for air flow, an inlet heat exchanger to acquire uniform and constant inlet temperature, a settling chamber and a contraction for uniform and high flow quality of air, a main test section and an exit chamber for measuring the air flow rate. Constant air temperature at the inlet of wind tunnel was maintained by circulating water between the inlet heat exchanger and a constant temperature water bath. The dimensions of the main test section were 315.0 mm wide, 29.2 mm high and 623 mm long, it had 100 mm long upstream chamber. In the exit chamber, a 22.2 mm diameter flow nozzle (ISA) was installed to measure the air flow rate. It was made according to the British Standard.[10]

Fig. 2 shows the configurations of a plane fin tested in the present work. The present test used the electrically heating element instead the hot water loop to evaluate the heat transfer performance of air side of heat ex-

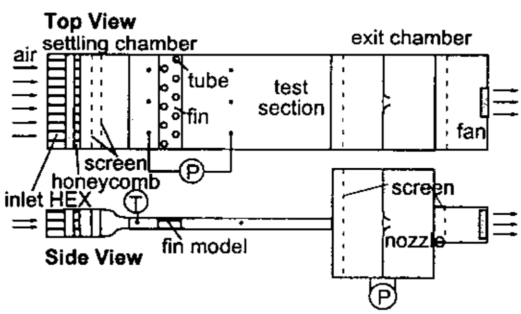

Fig. 1 Wind tunnel for 2 row-finned tube heat exchanger.

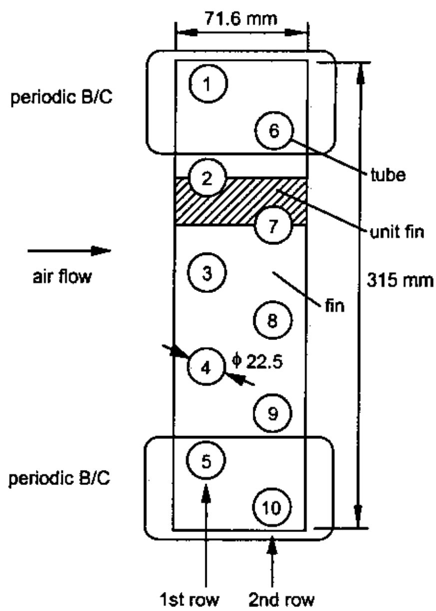

Fig. 2 Dimension and boundary condition along the width direction of enlarged model fin.

Table 2 Experimental conditions in the present test

Parameter	Test condition
types of fin	plane fin
scale factor	3 times of prototype
number of row	2 row
number of test fin	9 ea.
number of test tube	10 ea.
test fluid	air
frontal velocity	0.2~0.7 m/s

changer. A uniformly wound nichrome wire was installed inside the tube. Aluminum rings were used to simulate the tubes (usually copper tube) and the fin colors. The aluminum fins shown in Fig. 2 were inserted between the rings. The unit heat exchanger was stacked by nine fins and one hundred aluminum rings having 22.5 mm outer diameter. The unit model was tightly fixed at the end by bolts to reduce contact resistance. A 0.075 mm diameter of T type thermocouple was welded to the center aluminum ring to measure the wall temperature of the model. The overall dimensions and test condition are shown in Fig. 2 and Table 2. The test fin was made of 0.3 mm thick, 76.2 mm wide and 315 mm long aluminum plate and was three times enlarged in all dimensions. The total number of test tubes was ten, and they consisted of staggered alignment with two rows. Fin pitch, distance between fins, was 3.6 mm. Detailed dimension of the heat exchanger is listed in Table 3.

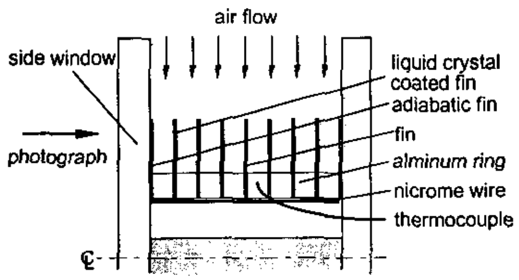

Fig. 3 Schematic diagram of installed heat exchanger.

Table 3 Dimensions of model fin in the present model test

Parameter	Dimensions
tube diameter (D)	22.5 mm
fin thickness (t)	0.30 mm
tube pitch (P_t)	63.0 mm
fin pitch (P_f)	3.63 mm
bare tube area (A_t)*	231 mm^2
fin surface area (A_f)*	4010 mm^2
total surface area (A_{tot})*	4240 mm^2
air volume between fins (V_c)*	6680 mm^3
area ratio (A_f/A_{tot})	17.0

* The dimension along the span-wise direction is for the hatched area of Fig. 2.

Fig. 3 shows a schematic diagram of installed heat exchanger. A fin at the side was painted by the liquid crystal (Hallcrest, R30-CW5) that the visible range was 30℃ to 35℃. The bare plane fin was carefully washed by alcohol and the black ink and liquid crystal was painted by the air blush. A plane fin made by a transparent ploycarbonate installed at the outside of the liquid crystal coated fin. An insulation window was installed at the outside.

2.3 Experimental method

The constant water bath and the inlet heat exchanger were operated after installing the heat exchanger model in the wind tunnel. Inlet temperature was the average of the temperature at six locations that had even control volume at the inlet cross section. Exit temperature was measured at two locations in the exit chamber. The temperatures were measured by T-type thermocouples that were calibrated within 0.1℃. Temperatures of all tubes can be assumed to be the same as that of a real operation. In the test model, each tube was electrically heated to have the same temperature by individual control. Six slidacses were used individually to obtain constant temperature conditions. Steady state was assumed if the differences among the tubes were less than 0.2℃ and the temperatures were maintained for more than 10 minutes. Temperature difference between the tube and the inlet was maintained more than 25℃ to enhance the sensitivity in the calculation of heat transfer coefficient. The heat transfer rates given by electric heater at each row were measured individually by the electric power meter (Voltech, PM300A) which had 0.1% accuracy.

The pressure drop in the sample heat exchanger and the flow nozzle was measured by a micro-manometer (Omega, PX653) calibrated within 0.1 Pa. We made the two sets of the static pressure taps flush on the wall of the test section. Each set consisted of six pressure holes. We measured the average pressure drop on the sample heat exchanger from each set of pressure taps. The air flow rate was calculated from the measured pressure differences at the flow nozzle. A micro-manometer with 0.1 Pa accuracy was used to measure the pressure drop. The mass flow rate at the flow nozzle was calibrated by means of a Pitot tube. The calibration agreed well with the equation given by the British Standard[10] within 0.3%. All of data was acquired and calculated by a data acquisition system (AOIP, SA32). The energy balance between electric heater and air side was less than 4% at the frontal velocity, $V_{fr} > 0.4$ m/s, and that was less than 5% at $V_{fr} < 0.4$ m/s.

The measured pressure drop consists of the net pressure drop, the entrance, the acceleration and the exit losses according to Kays and London.[11] The heat transfer coefficient corresponds to the definitions used in the wind tunnel test.

$$\frac{1}{UA} = \frac{1}{h_i A_i} + R_w + \frac{1}{\eta h A} \tag{1}$$

The surface efficiency is expressed as $\eta = A_{tube}/A + \eta_{fin} A_{fin}/A$. The U and h are the overall heat transfer coefficient and the pure heat transfer coefficient of the tube outside, i. e. 100% fin efficiency. We used the heat transfer coefficient multiplying surface efficiency, ηh, in the present work, since we do not know the fin efficiency or a theory for the strip fin efficiency. A_{fin}, A_{tube} and A denote the fin, tube and total surface areas, respectively. The heat transfer coefficient for each row defined in the equation (1) corresponds as followings.

$$Q = A\eta h \Delta T_{LM} \tag{2}$$

where the log-mean temperature differences, ΔT_{LM} is written as below.

$$\Delta T_{LM} = \frac{T_{ex} - T_{in}}{\ln(T_w - T_{in})/(T_w - T_{ex})} \tag{3}$$

The subscripts 'w', 'in' and 'ex' mean the tube wall, inlet and exit temperatures, respectively. The wall temperatures of each row were the average of the measured temperatures of the core tubes, and the exit temperatures of air were obtained by using the energy balance as below.

$$Q = \rho V_{fr} c_p (T_{ex} - T_{in}) \tag{4}$$

We did not use the measured exit temperature but the calculated exit temperature of above equation in the calculation for the log-mean temperature differences, equation (3). The Reynolds number is defined as $\mathrm{Re} = G_c D/\mu$, where $G_c = \rho V_{fr} A_{fr}/A_c$ in the present work. The A_{fr} and A_c are the frontal and the minimum cross-sectional areas, respectively.

The experimental method and procedure were as follows. The assembled heat exchanger model was installed in the wind tunnel. The

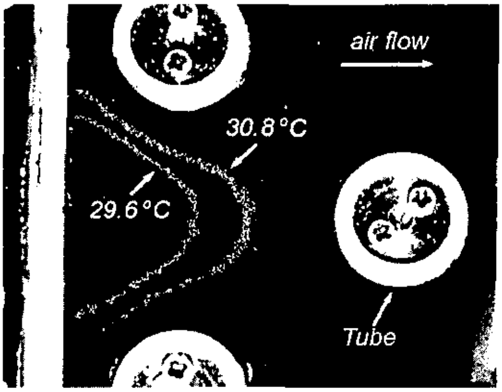

Fig. 4 Example of liquid crystal image.

measuring devices were operated and wormed-up. The temperature of water bath set as room temperature. The inlet air velocity and tube temperature were controlled by the fan speed and the output voltage of slidacs. The rigorous condition of the actual heat exchanger is the same in tube temperature. Therefore the tube temperatures were controlled by the six slidacs as the same temperature. The difference among the tube temperature was less than 0.3℃. The difference between inlet air and mean tube temperatures was set as about 20℃ at the test mode.

Light source and camera were fixed during the calibration and test modes. The liquid crystal was calibrated in the wind tunnel. The red color in the liquid crystal was the most sensitive. The reference picture was taken when the liquid crystal showed a uniform red color corresponded to the inlet temperature after 30 minutes operation without electric heating. Error of liquid crystal was less than 0.15℃ in this calibration. In the test mode we chose only the red color at six test runs by applying the temperature shifting method. The tube was electrically heated and inlet air temperature set as constant from 16℃ to 22℃. We could see a red contour on the fin surface. The temperatures of tube and air were shifted 1.0℃ at six test runs then we could see the red contour changed on the fin. In this test mode, the pictures were taken by the camera and the 480 by 640 digital image was obtained from the pictures by the scanner. RGB levels of the image were 256. The same procedure was conducted for the reference pictures. The location data were obtained from the images of the pictures of test mode by comparing the RGB values of the reference image. The tolerance of the RGB value was 4/256. An example of the iso-color points was shown in Fig. 4. Then we assign the temperature of the reference image to the location of the test pictures. The same procedures was conducted for the six test pictures and the data of the location-temperature were combined at a picture. The heat conduction in the fin was calculated by the finite difference method.

3. Results and discussions

3.1 Pressure and heat transfer

Fig. 5 and Fig. 6 show the pressure drop and heat transfer coefficient for the frontal velocity of three times enlarged model. The pressure drop reasonably agreed with the Grey and Webb[12] correlation. Their correlation was

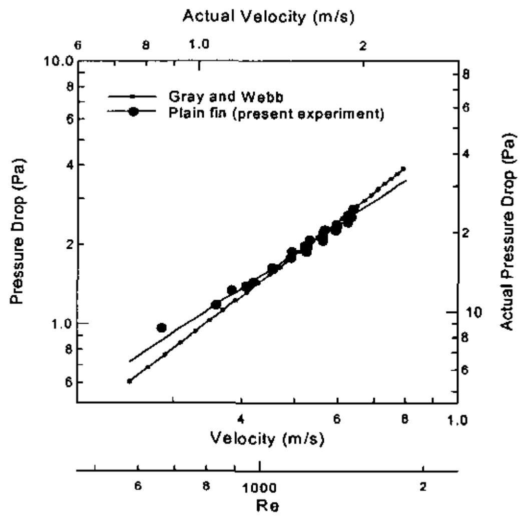

Fig. 5 Pressure drop of plain fin.

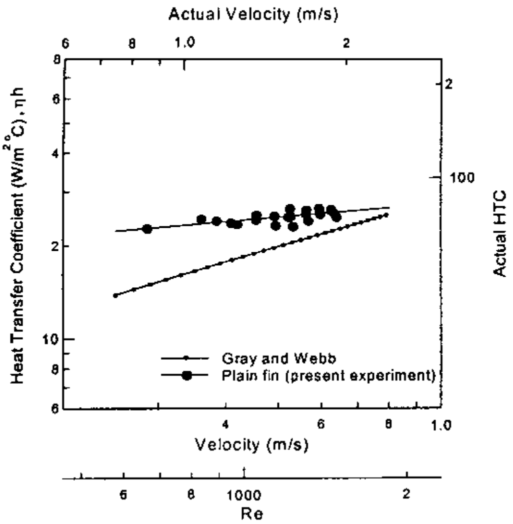

Fig. 6 Heat transfer coefficient of plain fin.

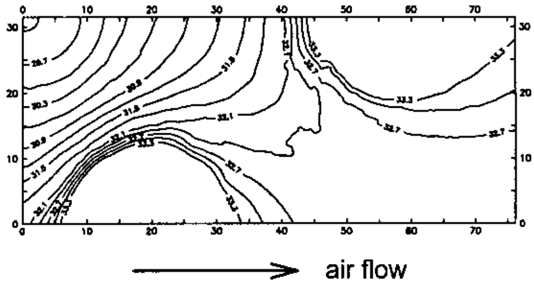

Fig. 7 Temperature distributions of plain fin (T_w=33.7℃, T_{in}=18.6℃, V_{fr}=0.64 m/s).

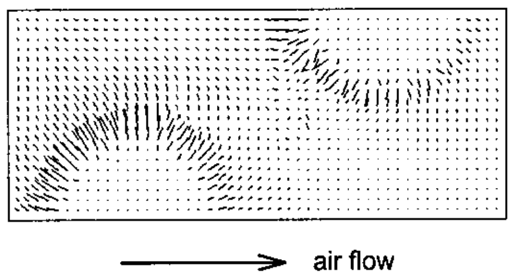

Fig. 8 Heat conduction in the plain fin (the same condition of Fig. 7).

less than the present experimental data at low frontal velocity and overestimated at the high frontal velocity. In heat transfer their correlation was considerably low at the low air velocity comparing the present experimental data. It is reason that their correlation was suggested for the high Re number (Re>2,400) and wide tube pitch ($(P_t/D)_{\text{present}}$=2.8, 1.97< $(P_t/D)_{\text{theory}}$<2.55). Wang et al.[13] also reported a similar results on the heat transfer of the plain fin. The correlation is need to be revised to use in the wide ranged of conditions. The present data was the ηh considered the fin efficiency.

3.2 Fin temperature and conduction

Fig. 7 shows a fin temperature distribution of the present three times model obtained by using the liquid crystal. Inlet and tube wall temperatures were 18.6℃ and 33.7℃ and frontal air velocity was 0.64 m/s. The temperature can be treated as the fin temperature because the fin thickness is thin as 0.3 mm. The fin temperature was increased along the flow direction because the air temperature increased. The temperature around the rear row was nearly uniform since the air temperature was saturated close to the tube temperature. The fin temperature between the front row tubes was low especially at the front fin edge. The temperature gradient near the tube was high especially at the front side of tube. The gradient behind of the tube was relatively low comparing than that front of tube. It is because of the wake of air flow behind of the tube. The local heat transfer would be low at that region. Fig. 8 shows the heat flux map calculated from the temperature fields. The heat conduction was far strong at the front row comparing the rear row. These experimental method and data could be applied to develop a high performance fin shape such as a strip fin.

4. Concluding remarks

The present work investigated the performance of the plane finned-tube heat exchanger having two row tubes. The pressure drop, heat transfer rate and temperature of fin were measured at the real operation conditions. We can conclude as follows from the present work.

(1) An experimental method was developed to measure the fin temperature distribution by using the liquid crystal.

(2) The Gray and Webb correlation for the plane fin was reasonably agree with the present experimental data. However the correlation for the heat transfer is needed to be revised.

(3) The quantitative information for the fin temperature was presented and the fin temperature of the rear row was nearly uniform at the actual operation condition.

(4) The heat conduction at the front row was far strong than that at the rear row and the local heat transfer behind the tubes was low.

References

1. Baggio, P. and Fornasicri, E., 1994, Air-side heat transfer and flow friction: theoretical aspects, in recent development in finned tube heat exchangers, Edited by Ch. Marvillet, DTI, Energy Technology, Denmark, pp. 91-159.
2. Goldstein, L. Jr. and Sparrow, E. M., 1976, Experiments on the transfer characteristics of a corrugated fin and tube heat exchanger configuration, J. of Heat Transfer, Vol. 98, pp. 23-34.
3. Beecher, D. T. and Fagan, T. J., 1987, Effect of fin pattern on the air-side heat transfer coefficient in plate finned-tube heat exchangers, ASHRAE Trans., Vol. 93, Part 2, pp. 1961-1984.
4. Ali, M. M. and Ramadhyani, S. 1992, Experiment on connective heat transfer in corrugate channels, Experimental Heat Transfer, Vol. 5, pp. 175-193.
5. Ito, M., Kimura, H. and Senshu, T., 1977, Development of high efficiency air-cooled heat exchanger, Hitachi Review, Vol. 26, pp. 323-327.
6. Kang, H. C. and Kim, M. H., 1999, Performance of material saved fin-tube heat exchanger in the dehumidifying condition, Proceedings of Autumn Annual Meeting of Society of Air-conditioning and Refrigeration Engineers of Korea, pp. 55-62.
7. Kim, K. S., 1993, An experimental study on the flow and heat transfer characteristics of an impinging jet, KSME J., Vol. 7, pp. 258-193.
8. Bunker, R. S., Metzger, D. E. and Witting, S., 1990, Local heat transfer in turbine disk-cavities, Part 1: roter and stator cooling with hub injection of coolant, Proceedings, ASME Gas Turbine and Aero-engine Congress, 90-GT-25.
9. Camci, C., Kim, K. and Hippensteele, S. A., 1992, A new hue capturing technique for the quantitative interpretation of liquid crystal images used in convective heat transfer studies, ASME J. Turbomachinery, Vol. 114, pp. 765-775.
10. British Standard Institution, 1964, Method for the measurement of fluid flow in pipes: Part 1: Orifice plates, nozzles and venturi tubes, British Standard 1042.
11. Kays, W. M. and London, A. L., 1984, Compact heat exchangers, 3rd ed., McGraw-Hill.
12. Gray, D. L. and Webb, R. L., 1980, Heat transfer and friction correlations for plate finned tube heat exchangers having plane fins, Proceedings, ASME, pp. 2745-2750.
13. Wang, C. C., Chen, P. Y. and Jang, J. Y., 1996, Heat transfer and friction characteristics of convex-louver fin-and-tube heat exchanger, Experimental Heat Transfer, Vol. 9, pp. 61-78.